

GUARANTEED INITIALIZATION OF DISTRIBUTED SPACECRAFT FORMATIONS*

Daniel P. Scharf,[†] Scott R. Ploen,[‡] Fred Y. Hadaegh,[§] Jason A. Keim,[¶] and Linh H. Phan[¶]

Jet Propulsion Laboratory
California Institute of Technology
Pasadena, CA 91009-8099

ABSTRACT

In this paper we present a solution to the formation initialization (FI) problem for N distributed spacecraft located in deep space. Our solution to the FI problem is based on a three-stage sky search procedure that reduces the FI problem for N spacecraft to the simpler problem of initializing a set of sub-formations. An analytical proof demonstrating that our algorithm guarantees formation initialization for N spacecraft constrained to a single plane is presented. An upper bound on the time to initialize a planar formation is also provided. We then demonstrate our FI algorithm in simulation using NASA's five-spacecraft Terrestrial Planet Finder mission as an example.

INTRODUCTION

Spacecraft formation flying has been identified as a critical technology for 21st century NASA astrophysical and Earth science missions. Specifically, formation flying refers to a set of distributed spacecraft that have the ability to interact and cooperate with each other and whose dynamic states are coupled through a control law. In deep space, formation flying enables variable-baseline interferometers that can probe the origin and structure of stars and galaxies with high precision. In addition, such interferometers will serve as essential instruments for discovering and imaging Earth-like planets orbiting other stars. Ultimately, the goal is to utilize distributed spacecraft interferometers to search for biosignatures in the atmospheres of extra-solar planets.

In order to accomplish these scientific objectives, interferometers with baselines that range from tens to tens of thousands of meters are required. The operation of such interferometers relies upon the ability of precision formation control systems to maintain relative spacecraft positions and orientations to an accuracy on the order of 1 centimeter and 1 arc minute, respectively, over large distances.

However, before precision formation coordination and control can occur, it is first necessary for each spacecraft to be able to communicate and to know the relative positions and velocities of one another. Although inertial position knowledge of each spacecraft is typically available, it cannot be used to determine relative states as it is not known to the required accuracy. Therefore, following initial spacecraft deployment or a fault condition, the spacecraft are "lost-in-space" (i.e., they are not communicating, and they do not know their relative positions and velocities). As a result, each spacecraft must perform a coordinated sky search to autonomously acquire relative state information. Here we assume that high accuracy inertial attitude information is available for each spacecraft from on-board star trackers.

The process of using on-board sensors to both establish communication among the formation members and to acquire the relative positions and velocities of the formation members is known as *Formation Initialization* (FI). Since formation acquisition sensors (e.g. AFF²) typically have limited fields-of-view, a search is necessary to acquire formation members; this search involves coupled translational and rotational maneuvers. Consequently, the FI problem becomes a formation guidance problem involving translational/rotational path planning and collision avoidance.

Although there has been previous work in the area of deep space formation flying guidance,³⁻⁷ the area of formation initialization is significantly underdeveloped. The work of Breckenridge and Ahmed⁸ at JPL focused on an initialization strategy for NASA's StarLight mission, which consisted of two spacecraft forming a variable baseline interferometer.

A number of major technical challenges must be overcome in order to realize a practical solution to the formation initialization problem for N distributed spacecraft. First, any candidate algorithm must guarantee formation initialization using limited field-of-view sensors. Second, formation attitude maneuvers must not violate sun-angle con-

[†]Staff Engineer, Member AIAA

[‡]Senior Engineer, Member AIAA

[§]Senior Research Scientist, Associate Fellow AIAA

[¶]Associate Engineer

*An overview of the algorithm presented herein previously appeared in Ref. 1.

straints.^{||} Further, any candidate FI algorithm must result in an efficient search procedure that mitigates the probability of collisions.

The remainder of this paper is organized as follows. In the next section we discuss in detail the challenges inherent in the N -spacecraft formation initialization problem. We then present a solution of the FI problem based on a coordinated, three-stage sky search procedure. Next, we discuss how our algorithm naturally leads to sub-formations and present the logic required to join these sub-formations. Then, since our solution to the FI problem involves a planar rotation of the formation spacecraft, we demonstrate analytically that our FI algorithm is guaranteed to initialize an N spacecraft formation constrained to a single plane in at most 1.5 revolutions. Next, we apply our FI algorithm to a realistic five spacecraft scenario using NASA’s Terrestrial Planet Finder (TPF) mission as a baseline and present some simulation results. Finally, we conclude and discuss some directions for future work.

THE FI PROBLEM

In this section we discuss the characteristics of the N spacecraft formation initialization problem. In this paper, formation initialization (FI) is defined as the process of using limited field-of-view, on-board sensors to establish communications among the formation members and to acquire the relative positions and velocities of the formation members.

The FI algorithm developed in the sequel is based upon a set of assumptions that are divided into the following categories: dynamic constraints, spacecraft/sensor characteristics and controller/estimator characteristics. We now discuss each category in detail.

Dynamic Constraints

We assume that each spacecraft in the formation is a rigid body in which the rotational and translational motions are decoupled. The number of spacecraft in the formation is arbitrary. Further, we assume that the spacecraft are located in deep space where disturbances such as gravity fields and aerodynamic effects are negligible. As a result, the free translational motion of the system consists of the center-of-mass of each spacecraft following a straight-line trajectory with constant velocity relative to an inertial observer.**

^{||}A typical imaging mission involves spacecraft carrying sensitive optical hardware that cannot withstand prolonged sun exposure. As a result, certain spacecraft attitudes are prohibited.

**Despite disturbances such as solar pressure, the motion of each spacecraft is approximately rectilinear over the time

Spacecraft/Sensor Characteristics

We assume that each spacecraft is equipped with a limited field-of-view Autonomous Formation Flying (AFF) sensor.² The AFF sensor functions as the “eyes” of the spacecraft by providing the means to measure inter-spacecraft (i.e., relative) positions. Specifically, the AFF is a GPS-like sensor consisting of one transmitter that emits a conical beam pattern with a central angle of $2\theta_{FOV}$ and three receivers with a combined reception pattern essentially identical to the transmission pattern. Inter-spacecraft range is determined from transmission delay, while phase differences between the three receiving antennas provide inter-spacecraft bearing angles.

The AFF is a distributed sensor; it requires a transmitter on one spacecraft and three receivers on another. Therefore, for the AFF sensor to function the spacecraft must each fall within the transmission/reception pattern of the other *simultaneously*. This configuration is referred to as a “front-to-front lock” or an F/F lock.

For the AFF sensors to obtain an F/F lock the following two constraints must *both* be satisfied

$$\theta_i = \arccos(\vec{b}_i \cdot \vec{e}_{ij}) \leq \theta_{FOV} \quad (1)$$

$$\theta_j = \arccos(\vec{b}_j \cdot \vec{e}_{ji}) \leq \theta_{FOV}. \quad (2)$$

Here \vec{b}_i denotes the AFF boresight vector (a unit vector along the centerline of the conical AFF beam pattern) of spacecraft i , denoted S/C_i , \vec{e}_{ij} denotes the unit vector from the center of the AFF on S/C_i to the center of the AFF on spacecraft j , denoted S/C_j , θ_{FOV} denotes the half-cone angle of the AFF antenna beam pattern, and \cdot denotes the standard Euclidean dot product. The angles θ_i and θ_j are shown in Fig. 1. See also Fig. 2. Further, the AFF antenna beam is assumed to have enough range for any FI scenario considered.

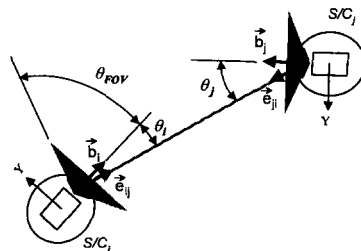


Figure 1: Geometric Variables in F/F Lock Constraints (1) and (2)

We also assume that each spacecraft is equipped with a functional omni-directional, inter-spacecraft communication (ISC) link, that there scale required to initialize the formation (a few minutes to an hour).

are no occlusions of the ISC, and that all inter-spacecraft communication is done instantaneously.^{††} Each spacecraft is also equipped with a sun-shield to protect sensitive optical hardware from direct sunlight. For the sun-shield to provide adequate protection, the attitude of each spacecraft is subject to certain sun-angle constraints. In particular, the sun-shield normal of each spacecraft must remain within a specified angle of the sun-line. Here we assume a constraint angle of 25° . To avoid beam distortion, the AFF is located at the edge of the sun-shield. Each spacecraft is further equipped with a star-tracker that provides accurate attitude knowledge. The maximum rotation rate of each spacecraft is limited due to star-tracker rate limitations. In the simulations to follow, we assume a maximum allowable angular rate of $0.25^\circ/s$. Finally, a body-fixed reference frame is affixed to the center of mass of each spacecraft with the x-axis pointing normal to the sun-shield, the z-axis along the AFF boresight, and the y-axis chosen to complete the right-handed triad. See Fig. 2.

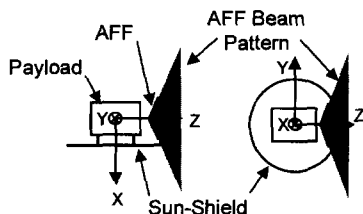


Figure 2: Body Frame and AFF Location for Generic Spacecraft

Controller/Estimator Characteristics

Each spacecraft is assumed to have full attitude and translational control capability. We further assume that all spacecraft maneuvers are performed kinematically (e.g. Δv 's are instantaneously delivered).^{††} Translational maneuvers are permitted without a direct relative state measurement available. Further, we assume that relative state knowledge, once acquired, does not significantly degrade over the period of FI.

Major Challenges of FI

Given the characteristics of the FI problem discussed above, we now summarize the major technical challenges inherent in initializing a set of distributed spacecraft:

^{††}These assumptions imply that inter-spacecraft communication is already established, thereby solving a portion of the initialization problem. If a limited-FOV ISC link is used (e.g. optical communication), then our initialization algorithm requires modification.

^{†††}This is equivalent to assuming that the formation control law has "infinite bandwidth."

1. FI must be accomplished for a set of N spacecraft using limited FOV Autonomous Formation Flying (AFF) relative position/velocity sensors.
2. A front-to-front (F/F) sensor lock must be registered before relative state information between two spacecraft is established. Typical AFF beam patterns and the F/F sensor lock geometry are shown in Fig. 1.
3. Certain spacecraft attitudes are prohibited due to sun-angle constraints.
4. FI must be accomplished in such a way that (i) the probability of spacecraft collisions is mitigated, and (ii) fuel consumption is not excessive.

In the next section we present a solution to the FI problem that addresses these issues.

FI ALGORITHM FOR N SPACECRAFT

In this section we present a methodology for initializing a set of N distributed spacecraft with limited FOV AFF sensors and arbitrary initial conditions. Our solution to the FI problem is based on a coordinated three-stage sky search consisting of (1) an in-plane search, (2) an out-of-plane search, and (3) a near field search. It is important to note that due to the F/F sensor lock requirement, a full 4π steradian sky search performed by each spacecraft is necessary but *not* sufficient to guarantee formation initialization.

In order to assure that the spacecraft see each other simultaneously during the sky search, the set of N spacecraft are first arbitrarily divided into two groups. The AFF boresights are set parallel within a group and anti-parallel (i.e., 180° out-of-phase) between groups. See Fig. 3 for an example of a 3:2 partition of a five-spacecraft initialization scenario. The two groups are denoted \mathcal{G}_A and \mathcal{G}_B in the sequel. Note that this decomposition of the set of spacecraft into two disjoint groups with anti-parallel AFF boresights is possible because the inertial attitude of all spacecraft is assumed known. We now discuss each stage of the coordinated sky search in detail.

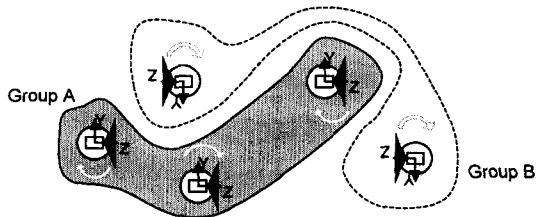


Figure 3: Decomposition of Five Spacecraft in Anti-Parallel Boresight Groups
In Plane Search (IPS)

The In-Plane Search (IPS) begins by dividing

the set of N spacecraft into \mathcal{G}_A and \mathcal{G}_B as discussed above. Then, the local body-fixed x -axes (normal to the sun-shield—see Fig. 2) of each spacecraft are pointed toward the sun. To complete the initial conditions for IPS, the spacecraft in \mathcal{G}_A point their z -axes in the same, arbitrary direction. Similarly, the spacecraft in \mathcal{G}_B point their z -axes in the direction anti-parallel to the arbitrary, z -axis direction of \mathcal{G}_A . Note that an attitude maneuver for each spacecraft is required to initialize IPS. Once all the spacecraft in \mathcal{G}_A and \mathcal{G}_B are properly oriented, each spacecraft begins rotating about its respective x -axis with constant angular rate Ω . The net effect is that the spacecraft perform synchronized rotations. See Fig. 3. The question immediately arises as to how many rotations each spacecraft should perform during IPS; we will demonstrate in the sequel that at most 1.5 revolutions are required.

The portion of the sky subtended by the AFF FOV during IPS for a single spacecraft is shown in Fig. 4. Note that the two shaded regions, called *complementary cones* (CC), are not searched during IPS. Referring to Fig. 4, if the half angle of the complementary cone is denoted θ_C , then the total solid angle subtended by both complementary cones is

$$\begin{aligned}\Psi_C &= 2 \int_0^{\theta_C} \int_0^{2\pi} \sin \theta d\phi d\theta \\ &= 4\pi(1 - \cos \theta_C),\end{aligned}\quad (3)$$

where θ and ϕ are the standard spherical coordinates. Recalling that a sphere subtends a full 4π steradians, the solid angle swept out by the AFF sensor in a full revolution is given by

$$\begin{aligned}\Psi &= 4\pi - \Psi_C \\ &= 4\pi \cos \theta_C.\end{aligned}\quad (4)$$

In this analysis we assume that $\theta_C = 20^\circ$; as a result, the AFF sensor for a single spacecraft subtends 94% of the sky during a single revolution.

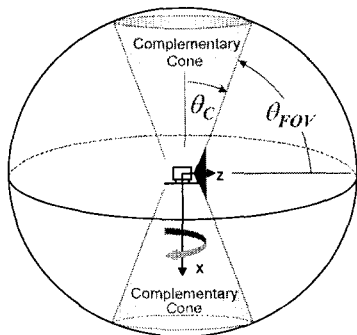


Figure 4: Sky Coverage During IPS

Summarizing, the IPS stage of the sky search consists of each group of spacecraft, \mathcal{G}_A and \mathcal{G}_B , per-

forming synchronized rotations about the sun-line with a fixed angular rate for 1.5 revolutions.

Out of Plane Search (OPS)

If after the 1.5 revolutions of IPS all N spacecraft have not found one another,* then the FI algorithm proceeds to the OPS mode. At this stage 94% of the sky has been searched by the groups \mathcal{G}_A and \mathcal{G}_B . The OPS mode is initialized by commanding each group of spacecraft to return to their initial IPS attitudes with an additional 180° rotation about the x -axis (boresights are still anti-parallel) with all angular rates nulled (i.e., $\Omega = 0$). If perfect control is assumed during IPS, then the start of OPS is identical to stopping all the spacecraft after the 1.5 revolutions of IPS.

The goal of the OPS stage is for each spacecraft to search its complementary cones. However, due to sun-angle constraints, unlimited rotations about the body y - and z -axes (see Fig. 2) are not permitted. Recall that we assumed the maximum allowable angle between the sun-shield normal (i.e., the x -axis) and the sun line is 25° and that the x -axis is initially aligned with the sun line. To search the two complementary cones under the 25° sun-angle constraint, all spacecraft from \mathcal{G}_A perform a 25° tip followed by a -50° tip about their body-fixed y -axes. Assuming that the half angle of the CC is $\theta_C = 20^\circ$ (See Fig. 4) it follows that the above attitude maneuver *does not* search out the entire 40° complementary cones.[†]

To complete the search of their CC's, each spacecraft in \mathcal{G}_A must rotate 180° about the sun line and then perform a 50° tip about the body y -axis.[‡] With the exception of the 180° sun-line rotation, it is critical that all attitude maneuvers done by spacecraft in \mathcal{G}_A are performed in the *opposite* direction by the spacecraft in \mathcal{G}_B . For example, when a spacecraft from \mathcal{G}_A tips 25° , a spacecraft in \mathcal{G}_B tips by -25° . See Fig. 5.

In summary, in the OPS stage of the sky search all spacecraft execute coordinated tips about the y -axis and rotations about the sun line to search

*The coordinated sky search is set up in such a way that spacecraft in \mathcal{G}_A can only acquire spacecraft in \mathcal{G}_B and vice versa. This *complementary* interaction between the two groups of spacecraft is an essential feature of our algorithm.

[†]We have assumed that it is not possible to temporarily relax the sun-angle constraint and search the entire 40° CC with a single attitude maneuver.

[‡]The tip angles required to fully cover the CC are given by $\alpha \triangleq \tan^{-1}(\cos \theta_{FOV} / \sqrt{1 - 2 \cos^2 \theta_{FOV}})$ and 2α (cf. 25° and 50° above). That is, for $\theta_{FOV} = 70^\circ$ the spacecraft must *initially* tip at least 21.3° to cover the CC. It is possible to specify values for θ_{FOV} and the sun constraint angle such that the CC cannot be fully searched.

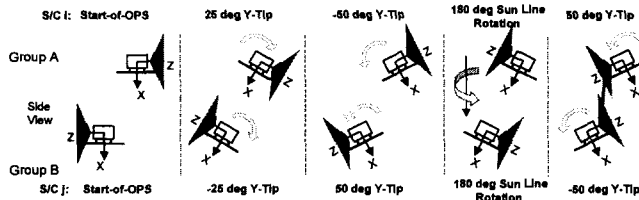


Figure 5: OPS Maneuvers for Spacecraft in Groups A and B

the complementary cones while maintaining the sun-angle constraint.

Near Field Search (NFS)

In the unlikely case that all the spacecraft have not been found, the FI algorithm proceeds to the Near Field Search (NFS). Since the AFF is located at the edge of the sun-shield, there exists an AFF to spacecraft center-of-mass offset.[§] The near field is defined as the unsearchable region adjacent to each spacecraft due to this offset. See Fig. 6.

The NFS search is initialized by commanding all spacecraft to return to their attitudes at the beginning of IPS with zero angular rate. The spacecraft then wait for a time $t^* = \frac{L}{v_{max}}$ where L is a characteristic near field length and v_{max} is an upper bound on initial relative translational rates. The purpose of waiting is to let the initial non-zero translational rates naturally let the spacecraft drift out of the near field. If there are still spacecraft that have not been acquired after waiting t^* seconds, then all remaining “lost” spacecraft are commanded to perform a translational maneuver in the anti-AFF bore-sight direction (i.e., along the $-z$ body-axis) with a Δv of magnitude $2v_{max}$.[¶]

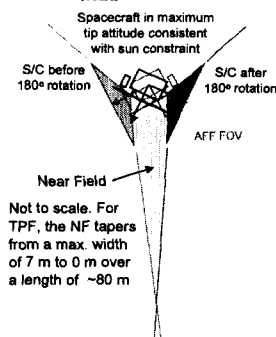


Figure 6: Geometry of Near Field

To summarize, the NFS stage of the sky search involves waiting for a time t^* , and then if needed, commanding an anti-boresight translational

[§]Recall that this offset is required to prevent the sun-shield from clipping the AFF signal.

[¶]This ensures that a spacecraft will not be trapped in the near field after the translational maneuver has been performed.

maneuver for all unacquired spacecraft.

If all spacecraft have not been found at the conclusion of the sky search, a fault condition is declared (e.g. a spacecraft may be out of range), and ground support is requested.

SUB-FORMATIONS AND JOIN LOGIC

In this section we discuss how the problem of initializing a set of N distributed spacecraft is reduced to one of joining a set of multi-spacecraft sub-formations. Here we define a *sub-formation* as a subset of two or more spacecraft that have obtained relative translational state knowledge as a result of an F/F lock. Sub-formations are a natural consequence of the temporal order inherent in initializing a set of $N > 2$ spacecraft.^{||} Using sub-formations, a formation is initialized in an aggregate manner, in much the same way as a complex molecule is constructed from simpler component atoms or as a crystal precipitates from solution.

We define the following two types of sub-formations:

1. **Formation Set (FS)** A FS is defined as a sub-formation that uses active control to maintain constant inter-spacecraft ranges. Spacecraft belonging to the FS behave as a virtual rigid body. The first two spacecraft that acquire one another in the FI process form the nucleus of the FS. Any other spacecraft that attains an F/F lock with a spacecraft in the FS is then brought into the FS by performing a suitable Δv to null its velocity relative to the FS.
2. **Knowledge Set (KS)** A KS is defined as a sub-formation in which no active control is used to maintain relative spacecraft positions. However, relative state knowledge is propagated to avoid collisions and for use in eventually joining sub-formations. The nucleus of a KS is formed when a second pair of spacecraft, neither associated with the FS, find one another. Any other spacecraft that attains an F/F lock with a spacecraft in a KS immediately joins that KS.

In order to conserve fuel, spacecraft in a KS do not perform translational maneuvers to null their relative velocities. The rationale is that spacecraft in a KS will eventually join the FS. To do so, these spacecraft will need to cancel their relative velocities with respect to the FS. Therefore, it is inefficient to impose an additional Δv to “rigidize” a KS. However, collision detection monitoring is performed within a KS, and if a collision is imminent, immediate corrective action is taken.

^{||}For example, spacecraft A first acquires spacecraft B, followed by spacecraft A or B acquiring spacecraft C, and so on.

All spacecraft not yet in a sub-formation are considered elements of the *Lost Set* (LS). The distinction between the FS and the KS is illustrated in the upper-left portion of Fig. 7.

We now discuss the logic required for joining a set of distinct sub-formations. The join logic used for a five-spacecraft scenario** is shown in Fig. 7. The join logic table in Fig. 7 is an exhaustive list of all possible scenarios for a formation with $N \leq 5$.

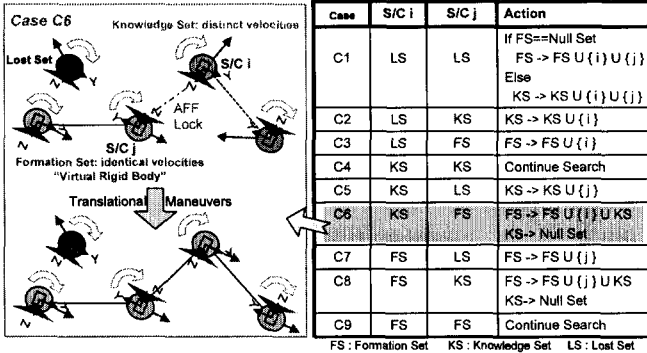


Figure 7: Join Logic Table for Sub-formations with Illustrated Example

As a representative example of the sub-formation join logic, consider Case 6 of Fig. 7. Here S/C_i in the KS and S/C_j in the FS attain an F/F lock. As a result, the formation set is enlarged to include S/C_i and all spacecraft in its associated knowledge set. To join the FS, all spacecraft in the KS perform a translational maneuver to null their velocities with respect to the FS. At the conclusion of these maneuvers, the five spacecraft consist of a four spacecraft FS moving as a virtual rigid body, and a single lost spacecraft yet to be acquired. The other eight scenarios listed in the join logic table can be described in a similar manner.

GUARANTEE OF IN-PLANE INITIALIZATION FOR N SPACECRAFT

In this section we present a proof demonstrating that a pair of spacecraft constrained to a given plane and using the initialization algorithm described in the previous sections attain an F/F lock in at most 1.5 revolutions. The proof immediately extends to an N spacecraft formation by considering a pair of spacecraft at a time.

Clearly, in a practical FI scenario all of the spacecraft are not constrained to a plane; the spacecraft each have a full six degrees of freedom (DOF). For the full 6 DOF FI problem, it is straightforward to show that the coordinated three-stage sky search

**Although we have assumed $N = 5$, this is not a restrictive assumption as the join logic can be readily scaled to arbitrary N . The difference is that multiple knowledge sets can occur when $N > 5$.

presented previously guarantees formation initialization in the static case.^{††} As a step toward the general proof of non-static 6 DOF FI, this section provides a proof guaranteeing initialization for non-static 3 DOF (i.e., two translational and one rotational DOF) FI.

Note that the 3 DOF, non-static proof directly applies to the 6 DOF non-static FI case when spacecraft relative velocities do not carry one spacecraft in the complementary cone of another. The challenge in extending the 3 DOF proof to the 6 DOF case is due to the possibility that a spacecraft may move into or out of a complementary cone during IPS.

Concentrating on the 3 DOF, non-static case, the assumptions for the proof are as follows:

- A1. S/C_i and S/C_j do not have *a priori* knowledge of their relative range and bearing.
- A2. No collisions occur.
- A3. The AFF of S/C_i is located at the spacecraft's center of mass (COM).^{††}
- A4. The motion of the system is described relative to an observer fixed to S/C_i and translating with S/C_i . This observer is a valid inertial frame of reference.* Without loss of generality, S/C_i is assumed fixed at a point O and S/C_j moves with constant velocity $\vec{v} = \vec{v}_j - \vec{v}_i$ relative to S/C_i , where \vec{v}_i and \vec{v}_j denote the absolute velocities of each spacecraft. An inertial frame of reference, denoted $\mathcal{F}_I = \{\vec{n}_1, \vec{n}_2, \vec{n}_3\}$, is affixed to S/C_i at point O .
- A5. The relative position vector of S/C_j with respect to S/C_i is constrained to the plane spanned by \vec{n}_1 and \vec{n}_2 .
- A6. Without loss of generality, the initial boresight direction of S/C_i is aligned with \vec{n}_1 .
- A7. The attitude of S/C_j is initialized so that its AFF sensor boresight is antiparallel to that of S/C_i (i.e., in the $-\vec{n}_1$ direction).
- A8. Each spacecraft is rotating with a constant angular velocity of $\vec{\Omega} = \Omega \vec{n}_3$, where $\Omega > 0$.

The geometry of the 3 DOF, non-static FI problem is shown in Fig. 8. The vector $\vec{R} = R\vec{e}_R$ points from S/C_i to S/C_j . The vector $\vec{\rho} = \rho\vec{e}$ is fixed in \mathcal{F}_I and describes the position of S/C_j relative to

^{††}By static we mean that all spacecraft relative velocities are initially zero.

^{††}This assumption is a valid approximation when the spacecraft separation is significantly larger than the size of the spacecraft. Further, this assumption can be relaxed to only requiring that the AFF boresight be aligned with the vector from the spacecraft COM to the AFF.

*The only translational maneuvers occur after an F/F lock. This analysis only considers the time up to this lock.

where k is an integer.

The lemma presented next is used in conjunction with the condition (12) to prove that an F/F lock is obtained in at most 1.5 revolutions.

Lemma 1 *Let f and g be continuous functions from the interval $[u, v]$ to \mathcal{R} . If there exist two points in $[u, v]$, t_1 and t_2 , such that $f(t_1) \geq g(t_1)$ and $f(t_2) \leq g(t_2)$, then f and g intersect between t_1 and t_2 .*

Proof: The lemma follows from an application of the Intermediate Value Theorem and the continuity of the function $f - g$. See Ref. 9, pages 165 and 170. \square

The main result of this section is the following theorem.

Theorem 1 *Two spacecraft confined to a plane that meet assumptions A1-A8 will obtain an F/F lock in at most 1.5 revolutions.*

Proof: A revolution is defined as $2\pi/\Omega$ seconds. Let t^* be one of the times at which condition (12) is satisfied. We must show that there exists a $t^* \leq 3\pi/\Omega$.

The proof is based on the observation that \mathcal{H} is the sum of \mathcal{A} and \mathcal{B} . Therefore, the angles of these phasors bound γ , the angle of their sum. To show that (12) is satisfied within 1.5 revolutions, we will first show that γ is continuous. Then using the bounds on γ provided by $\angle\mathcal{A}$ and $\angle\mathcal{B}$ and the properties of continuous functions, we will show that $\gamma = k2\pi$ for some integer k at a time $t^* \leq 3\pi/\Omega$.

We first show that γ is a continuous function for $t \geq 0$ when there are no collisions.

Recalling $|\mathcal{H}| = 1$, and in reference to Fig. 9, γ may be expressed as

$$\gamma(t) = \begin{cases} \Omega t - \theta - \pi/2 + \text{sgn}(A(t)) \cos^{-1}(|B(t)|), & \text{if } B(t > 0) \geq 0 \\ \Omega t - \theta + \pi/2 - \text{sgn}(A(t)) \cos^{-1}(|B(t)|), & \text{if } B(t > 0) < 0 \end{cases} \quad (13)$$

In either case of (13), the first three terms on the right-hand side equal $\angle\mathcal{B}$. The difference in sign between the two cases for the fourth term is due to the fact that when $A(t) > 0$ and $B(t > 0) \geq 0$, then \mathcal{A} is to the left (i.e., rotated counter-clockwise) of \mathcal{B} . Similarly, when $A(t) > 0$ and $B(t > 0) < 0$, then \mathcal{A} is to the right (i.e., rotated clockwise) of \mathcal{B} .

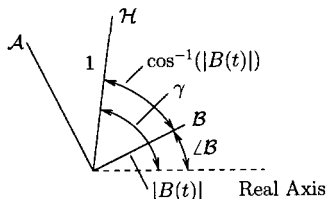


Figure 9: Calculating γ for $A(t) > 0$, $B(t) > 0$

Certainly, Fig. 9 does not prove the validity of (13). However, a figure may be drawn for each of

the ten possible combinations of signs of $A(t)$ and $B(t)$.[†] Enumerating the formulas for γ , $\angle\mathcal{A}$ and $\angle\mathcal{B}$ in each case then demonstrates the correctness of (13).

We now argue that $\gamma(t)$ is continuous for $t \geq 0$ based on (13). Since there are no collisions, $\Delta \neq \pi$. Hence, d never equals 0, and therefore $B(t)$ is continuous. Also, note that $\cos^{-1}(\cdot)$ is continuous on the domain $[0, 1]$, which is the case here.[‡] Assuming that $A(t)$ does not change sign, $\gamma(t)$ is the composition of continuous functions and so is itself continuous.

Now assume $A(t)$ changes sign. From (10) we observe that $A(t)$ is continuous when $\Delta \neq \pi$; further, $A(t)$ is initially positive and can change sign at most once. Let $\hat{t} > 0$ be the unique time when $A(t) = 0$. Note that $\cos^{-1}(|B(t)|)$ is still continuous and that $\cos^{-1}(|B(\hat{t})|) = 0$. Without loss of generality, consider the upper branch of (13). To show that γ is continuous, we show $\lim_{t \rightarrow \hat{t}^-} \gamma(t) = \gamma(\hat{t})$.

When approaching \hat{t} from the left, $A(t) > 0$ and so $\text{sgn}(A(t)) = 1$. Hence, $\lim_{t \rightarrow \hat{t}^-} \gamma(t) = \lim_{t \rightarrow \hat{t}^-} \gamma(t) |_{\text{sgn}(A(t))=1}$. Similarly, $\lim_{t \rightarrow \hat{t}^+} \gamma(t) = \lim_{t \rightarrow \hat{t}^+} \gamma(t) |_{\text{sgn}(A(t))=-1}$. In both cases the limit equals $\Omega\hat{t} - \theta - \pi/2$, which is $\gamma(\hat{t})$. Therefore, $\gamma(t)$ is continuous.

Now, $\angle\mathcal{A}$ and $\angle\mathcal{B}$ will be used to provide upper and lower bounds on γ . Then, from examining the times at which these bounds equal $k2\pi$, the first time γ equals $k2\pi$ can be bounded. To this end, Lemma 1 will be invoked to show that if the upper and lower bounds equal $k2\pi$ at times t_1 and t_2 , respectively, then γ must equal $k2\pi$ for some t such that $t_1 \leq t \leq t_2$.

In bounding γ with $\angle\mathcal{A}$ and $\angle\mathcal{B}$, there are two cases to consider: 1) $A(t)$ does not change sign, and 2) $A(t)$ does change sign.

If $A(t)$ does not change sign, then depending on the sign of $B(t)$, \mathcal{H} lies between 90° to the right (i.e., rotated clockwise) of \mathcal{A} and 90° to the left (i.e., rotated counter-clockwise) of \mathcal{A} . That is, an upper bound for γ is $\bar{\gamma} = \angle\mathcal{A} + \pi/2$, and a lower bound is $\underline{\gamma} = \angle\mathcal{A} - \pi/2$. Since $\sigma_A = 0$ when $A(t)$ does not

[†]First, $A(t)$ and $B(t)$ cannot be simultaneously zero. If $A(t)$ is zero, then $B(t)$ is either positive or negative. If $A(t)$ is positive, then $B(t)$ can be negative, positive, zero-always, zero-initially-then-positive, or zero-initially-then-negative. Due to the definition of σ_B , the cases $B(t)$ is zero-always and $B(t)$ is zero-initially-then-positive can be treated as the same case. Hence, there are four cases for $A(t)$ positive. Similarly, there are four cases for $A(t)$ negative.

[‡]Since \mathcal{A} and \mathcal{B} are orthogonal, the magnitude of \mathcal{H} is always greater than or equal to the magnitude of \mathcal{B} . Since the magnitude of \mathcal{H} is 1, the magnitude of \mathcal{B} can never be greater than 1.

change sign, we have

$$\bar{\gamma}(t) = \Omega t - \theta + \pi/2 \quad (14)$$

$$\underline{\gamma}(t) = \Omega t - \theta - \pi/2. \quad (15)$$

We now prepare for application of Lemma 1. First, we must select a value for k . Note that $\bar{\gamma}(0) \in (-3\pi/2, \pi/2]$. Consider the case when $\bar{\gamma}(0) \leq 0$. This inequality implies $\theta \in [\pi/2, 2\pi)$. Since $\bar{\gamma}$ is strictly increasing and $\bar{\gamma}(0) \leq 0$, the first time $\bar{\gamma} = k2\pi$ is for $k = 0$. From (14), this equality occurs at $t_1 = (\theta - \pi/2)/\Omega$. Similarly, $\underline{\gamma} = 0$ at $t_2 = (\theta + \pi/2)/\Omega$.

We now have $\gamma \leq \bar{\gamma} \leq 0$ for $t \leq t_1$ and $\gamma \geq \underline{\gamma} \geq 0$ for $t \geq t_2$. Define $f(t) \equiv 0$ and $g(t) \triangleq \gamma(t)$. By Lemma 1, there exists a time $t^* \in [t_1, t_2]$ such that f and g intersect. That is, there is a time $t^* \leq t_2$ such that $\gamma(t^*) = 0$. Since $\theta \in [\pi/2, 2\pi)$, we have $t^* \leq t_2 < (5/2)\pi/\Omega$.

Now consider the case when $\bar{\gamma}(0) > 0$. This inequality implies $\theta \in [0, \pi/2)$. The first time $\bar{\gamma}$ equals $k2\pi$ in this case is for $k = 1$. For $k = 1$, we have $\bar{\gamma} = 2\pi$ at $t_1 = ((3/2)\pi + \theta)/\Omega$ and $\underline{\gamma} = 2\pi$ at $t_2 = ((5/2)\pi + \theta)/\Omega$. Applying Lemma 1 in a similar manner, there exists a time $t^* \leq t_2$ such that $\gamma(t^*) = 2\pi$. Since $\theta \in [0, \pi/2)$, we have $t^* \leq t_2 < 3\pi/\Omega$.

Now consider the case when $A(t)$ changes sign. Whether $B(t > 0) > 0$ or $B(t > 0) < 0$,[§] \mathcal{H} is bounded between 90° to the left (i.e., clockwise) and 90° to the right (i.e., rotated counter-clockwise) of \mathcal{B} . That is, $\bar{\gamma} = \angle B + \pi/2$ and $\underline{\gamma} = \angle B - \pi/2$.

If $B(t > 0) > 0$, then $\angle B = \Omega t - \theta - \pi/2$. Therefore, $\bar{\gamma}(t) = \Omega t - \theta$ and $\underline{\gamma}(t) = \Omega t - \theta - \pi$. Note that $\bar{\gamma}(0) \in (-2\pi, 0]$ and so we need only consider $k = 0$. We have $t_1 = \theta/\Omega$ and $t_2 = (\theta + \pi)/\Omega$. Following a similar argument as for the previous cases, there exists a $t^* \leq t_2$ at which $\gamma(t^*) = 2\pi$. Since $\theta \in [0, 2\pi)$, we have $t^* < 3\pi/\Omega$.

A similar argument for the case when $B(t > 0) < 0$ shows there exists a $t^* \leq t_2 < 3\pi/\Omega$.

Taking the maximum of the t^* 's for each case, the spacecraft see each other within $3\pi/\Omega$ seconds, which corresponds to 1.5 revolutions. \square

APPLICATION TO TPF MISSION AND SIMULATION RESULTS

In this section we apply the FI algorithm to the five spacecraft formation of the Terrestrial Planet Finder (TPF) mission and present simulation results for this application.

First, using the join logic discussed previously, all possible FI scenarios for TPF can be enumerated using a directed graph. The key aspect of

[§]Since A and B cannot be simultaneously zero, if A changes sign, then $B(t > 0) \neq 0$.

this directed graph is that spacecraft are numbered corresponding to the temporal order in which they achieve F/F lock. For example, if the spacecraft are labeled A through E, and spacecraft C and E achieve the first F/F lock, then they become spacecraft 1 and 2, respectively. Next, if C and A achieve an F/F lock, then A becomes spacecraft 3. The advantage of this labeling convention is that it reduces the number of possible permutations, thereby greatly simplifying the graph.

The FI directed graph for TPF is shown in Fig. 10. It is a tree directed graph progressing from left to right. At the ‘‘Start’’ all spacecraft are lost-in-space. Next, as indicated by the branching arrows, either two spacecraft achieve an F/F lock, become spacecraft 1 and 2 and form the formation set, or the entire FI algorithm is completed with no F/F locks. In this case, a fault is declared. The fact that spacecraft 1 and 2 form a formation set is indicated by a solid arrow. Continuing from $1 \rightarrow 2$, there are three possibilities. First, there may be no new F/F locks and a fault is declared. Second, two other spacecraft may achieve an F/F lock; since a formation set already exists, these two spacecraft form a knowledge set. A knowledge set is indicated by a dashed arrow. Finally, either spacecraft 1 or 2 may achieve an F/F lock with a third spacecraft. In this case, as shown by $(1 \rightarrow 2) \rightarrow 3$, spacecraft 3 joins the formation set. The ‘‘or’’ is indicated by the parentheses. For example, $(1 \rightarrow 2) \rightarrow (3 \rightarrow 4 \rightarrow 5)$ is read as spacecraft 1 or 2 of the formation set sees spacecraft 3, 4 or 5 of the knowledge set and spacecraft 3, 4 and 5 join the formation set.

The shaded path in Fig. 10 is the scenario that occurs in the TPF FI simulation presented next.

The formation initialization algorithm is demonstrated in simulation for five spacecraft. Each spacecraft has a 15 m diameter sun-shield and a single AFF sensor located on the edge of its sun-shield.[¶] A 7.5 m AFF offset from the spacecraft center of mass produces a near-field with a characteristic length of 80 m . The AFF sensor half-cone angle is taken to be 70° . The spacecraft processor runs at 1 Hz. We reiterate that the simulation is kinematic, that is, perfect control is assumed. However, the FI guidance algorithm will eventually be integrated into a high-fidelity, kinetic simulation as part of a complete formation mission demonstration.

The spacecraft are initially separated by up to 300 m with relative speeds of up to 12 cm/s . The initial conditions were chosen to ensure that the OPS stage is entered.

[¶]The sun-shield is modeled as part of the spacecraft rigid body.

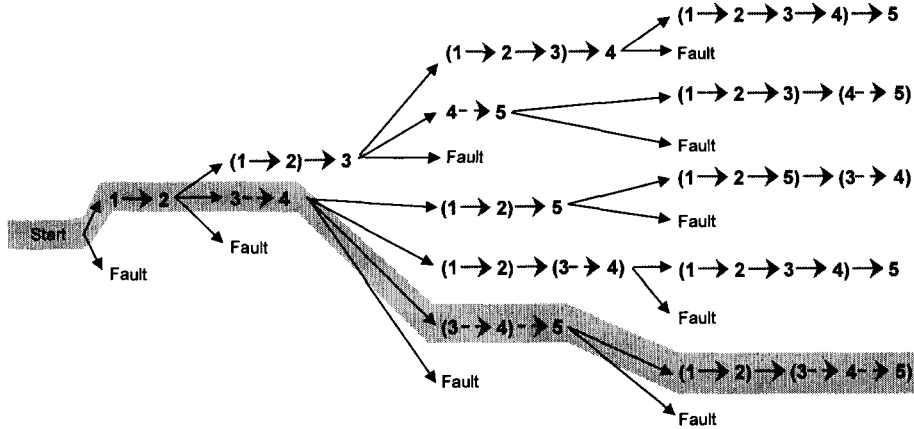


Figure 10: TPF FI Directed Graph

The FI algorithm simulated is a slight variant on the algorithm presented in this paper. The IPS stage consists of only one revolution of the spacecraft, not 1.5 revolutions.

The results of the simulation are shown using a three view format. See Fig. 11. The upper right window, called the Sun View, shows the spacecraft as viewed from the Sun. Note that only their sunshields and the solar panels can be seen. The lower right window, called the Spacecraft View, is a close-up of one spacecraft. The maneuvers that comprise the three stage sky search are most easily seen in this view. The Oblique View is an overall view of the formation. Grey cones represent each spacecraft's AFF FOV. Finally, the time elapsed and the current stage of the sky search are shown in the upper right.

At the beginning of the simulation, all spacecraft align their x-axes with the Sun. The z-axes (AFF boresights) are then aligned according to assignments in \mathcal{G}_A or \mathcal{G}_B . After this initial alignment, IPS commences. At approximately twelve minutes, as shown in Fig. 11, the bottom two spacecraft shown in the Oblique View see one another. A line joining the spacecraft indicates an F/F lock. Since these are the first two spacecraft to attain an F/F lock, they become the nucleus of the formation set. Subsequently, both spacecraft in the formation set will be traveling through space as a virtual rigid body. The white lines trailing each spacecraft indicate their inertial translational motions.

At 14 minutes the upper two spacecraft in the Oblique View of Fig. 11 see one another and form a knowledge set. There are now two sub-formations consisting of two spacecraft each.

At approximately 16 minutes, as shown in Fig. 12, a spacecraft in the knowledge set sees the last lost spacecraft. The lost spacecraft immediately joins the knowledge set. The upper three spacecraft of the Oblique View now comprise a knowledge set

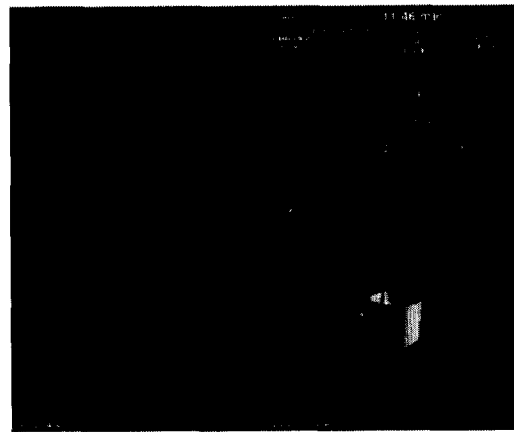


Figure 11: TPF FI Simulation at 12 Minutes.

and the bottom two spacecraft comprise the formation set. Note the kink in the white trail of the spacecraft second from the bottom of the Oblique View in Fig. 12. The kink corresponds to the translational maneuver that was necessary to form the formation set.

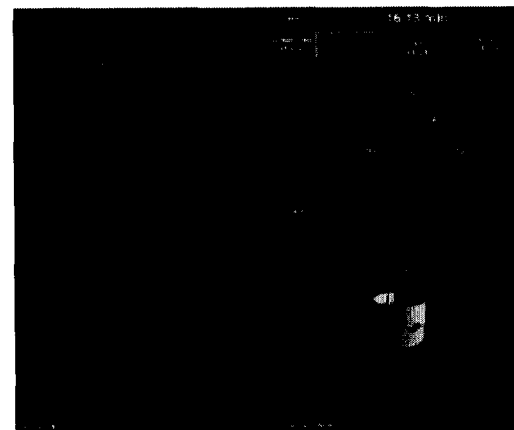


Figure 12: TPF FI Simulation at 16 Minutes.

At 24 minutes IPS is complete and no new F/F locks have occurred. Since the formation set does not contain all five spacecraft, OPS is initi-

ated. During the first tip of 50° in OPS, a spacecraft in the knowledge set and a spacecraft in the formation achieve an F/F lock. This F/F lock is shown the Oblique View of Fig. 13 as a long diagonal line. As can be seen in the Sun View, some of the spacecraft have tipped their AFF cones towards the reader, while others have tipped their cones away. This F/F lock between the knowledge and formation sets occurs at 28 minutes and 40 seconds. After the appropriate translational maneuvers to null relative velocities, the formation is fully initialized. Since the formation has been completely initialized during the Out-of-Plane stage, the Near-Field stage is not required.



Figure 13: TPF FI Simulation at 29 Minutes.

CONCLUSION

In this paper we have developed an algorithm for initializing a set of N distributed spacecraft located in deep space. Our solution to the formation initialization problem is based on a three-stage sky search procedure consisting of (1) an in-plane search, (2) an out-of-plane search, and (3) a near field search. Moreover, realistic mission constraints such as limited FOV AFF sensors and sun-angle restrictions are explicitly considered. Another important feature of our solution is that the FI problem for N spacecraft is naturally reduced to the simpler problem of initializing a set of sub-formations. We then presented an analytical proof demonstrating that our algorithm guarantees formation initialization in at most 1.5 revolutions for N spacecraft constrained to a given plane, and discussed the challenges in extending this proof to guarantee 6 DOF, non-static FI. Finally, we demonstrated the performance of our algorithm in simulation by using NASA's five spacecraft Terrestrial Planet Finder mission as a baseline. In less than a half hour all five spacecraft were acquired. During Monte Carlo simulations, FI was typically completed during IPS, that is, in less than 24 minutes, and no failures of the

algorithm occurred. Motivated by these results, future work is aimed at reducing the conservatism in the 1.5 revolution bound and extending the planar initialization proof to FI with arbitrary spacecraft initial conditions.

ACKNOWLEDGEMENTS

This research was performed at the Jet Propulsion Laboratory, California Institute of Technology, under contract with the National Aeronautics and Space Administration. The authors would like to gratefully acknowledge William Breckenridge and Asif Ahmed of JPL and Prof. Marwan Bikdash of North Carolina A&T University for their valuable contributions to the work described in this paper.

REFERENCES

- [1] F.Y. Hadaegh, D.P. Scharf, and S.R. Ploen, "Initialization of distributed spacecraft for precision formation flying," in *IEEE Conf. Control Applications*, Istanbul, Turkey, June 2003.
- [2] S.-C. Wu and D. Kuang, "Positioning with Autonomous Formation Flyer (AFF) on Space-Technology 3," in *ION GPS*, Nashville, TN, 1999.
- [3] D. P. Scharf, F. Y. Hadaegh, and S. R. Ploen, "A survey of spacecraft formation flying guidance and control (part I): Guidance," in *American Control Conf.*, Denver, June 2003.
- [4] D. P. Scharf, F. Y. Hadaegh, and B. H. Kang, "On the validity of the double integrator approximation in deep space formation flying," in *Int. Symp. on Formation Flying Missions & Technologies*, Toulouse, France, Oct. 2002.
- [5] G. Singh and F. Y. Hadaegh, "Collision avoidance guidance for formation-flying applications," in *AIAA Guidance, Navigation, and Control Conf.*, Montreal, Canada, Oct. 2001.
- [6] S. Li, R. Mehra, R. Smith, and R. Beard, "Multi-spacecraft trajectory optimization and control using genetic algorithm techniques," in *Proc. IEEE Aerospace Conf.*, Big Sky, MT, pp. 99–108, Mar. 2000.
- [7] F.Y. Hadaegh, G. Singh, M. Quadrelli, and J. Shields, "Modeling and control of formation flying spacecraft in deep space and earth orbits," in *Workshop on Terrestrial Planet Finder*, Jet Propulsion Laboratory, Pasadena, CA, 2000.
- [8] W. E. Breckenridge and A. Ahmed, "StarLight AFF acquisition strategy." JPL Internal Memorandum, April 30, 2001.
- [9] S.R. Lay, *Analysis with an Introduction to Proof*. Englewood Cliffs, NJ: Prentice-Hall, Inc., 2 ed., 1990.